Neural Computing and Applications
https://doi.org/10.1007/s00521-018-3614-y

S.I. : EMERGING INTELLIGENT ALGORITHMS FOR EDGE-OF-THINGS COMPUTING

Computer-based Cobb angle measurement using deflection points in adolescence idiopathic scoliosis from radiographic images

Areen K. Al-Bashir[1] · Mohammad A. Al-Abed[2] · Hala K. Amari[1] · Fadi M. Al-Rousan[3] · Omar M. K. Bashmaf[3] · Enas W. Abdulhay[1] · Rabah M. Al Abdi[1] · N. Arunkumar[4] · B. R. Tapas Bapu[5] · Ahmad K. Al-Basheer[6]

Received: 23 April 2018 / Accepted: 25 June 2018

Abstract
Idiopathic scoliosis treatment depends on the accurate assessment of the Cobb angle, which is usually performed manually. Manual measurements, however, can lead to observer variations, which depend on the correct selection of the curvature superior and inferior vertebrae in order to draw the needed lines for Cobb angle measurements. In this paper, we are proposing an algorithm to measure the Cobb angle semi-automatically. The algorithm is based on two processing phases in which each column in the raw X-ray image is reduced to two points representing the end points of the spine and containing its general structure and outline. These points are then used to fit a fifth-order polynomial. We hypothesize that the deflection points of the fitted curve represent the superior and inferior vertebrae of the scoliosis curvature. The deflection points were used to calculate the Cobb angle. The algorithm was tested on X-ray images from 28 subjects (14 females and 14 males, average age of 15.6 ± 1.3 years) diagnosed with adolescence idiopathic scoliosis. Three manual measurements were obtained, with manually measured Cobb angles ranging from of 10° to 98°. The mean of the standard deviation of the manual readings and the algorithm results was 5.28° and 2.64°, respectively, with mean abs error of 6.6° and R value of 0.81. Excluding the cervical and rib cage touching scoliosis cases, the mean of the standard deviation of the manual readings and the algorithm results was 4.73° and 2.35°, respectively, with mean abs error of 3.78° and R value of 0.94. From the results, we can conclude that our proposed algorithm can minimize and simplify user intervention, thus allowing easier and more accurate Cobb angles measurements and resulting in a shorter diagnosis time and requiring no special skills from the user.

Keywords Adolescence idiopathic scoliosis · Digital radiography · Deflection points · Cobb angle · Automation

1 Introduction

Idiopathic scoliosis (IS) is defined as three-dimensional torsional deformity of the spine column, generally characterized by a lateral deviation of the spine, combined with variable degrees of rotational as well as translational deformity of the spine [1–5]. Diagnosis of the deformity is usually done by a standing radiograph of the spine, which is regarded as the gold standard for the diagnosis and monitoring of such cases. From these radiographs, a Cobb's angle can be obtained [1, 6, 7], which is defined as the angle formed between a line drawn through the upper part of superior vertebrae and a second line drawn through the lower part of inferior vertebrae, and this angle is used to evaluate the degree of lateral curvature of the spine [1, 6, 8]. A Cobb angle larger than 10° is considered clinically significant for the diagnosis of IS [1, 5].

✉ Areen K. Al-Bashir
akbashir@just.edu.jo

[1] Biomedical Engineering Department, Jordan University of Science and Technology, P. O. Box 3030, Irbid 22110, Jordan

[2] Biomedical Engineering Department, the Hashemite University, Zarqa 13133, Jordan

[3] Orthopedic Department, Jordanian Royal Medical Services, Amman 11855, Jordan

[4] Department of Electronics and Instrumentation, Sastra University, Thajavur, India

[5] Faculty of Electronics and Communication Engineering, S.A. Engineering College, Chennai, India

[6] Radiation Oncology Department, Medical College of Georgia, Augusta, GA 30912, USA

Published online: 30 June 2018

Cases of IS, in which there is no identifiable underlying cause, represent 80–85% of all diagnosed scoliosis cases [1, 2, 9, 10]. This type of scoliosis could be further classified according to the age of diagnosis into three major groups. Infantile idiopathic scoliosis, in which diagnosis is done before 3 years of age, juvenile idiopathic scoliosis, when diagnosed between 3 and 10 years, and the adolescent idiopathic scoliosis (AIS) type in which diagnosis is done between 10 and 18 years [1, 2]. If diagnosed above the age of 18 years, it is classified as adult idiopathic scoliosis [1, 6].

While several large-scale surveys identify a wide range of occurrence of IS diagnosis from as low as 0.5% up to 12% of Cobb angle above 10° [1, 9], AIS represents most of the diagnosed cases and is generally described to have 2–3% prevalence in the age group of 10–18 years of age [6, 10, 11]. Females are more susceptible to AIS occurrence compared to males [1, 9, 12] with a ratio of 2:1, which increases with age. If left untreated, scoliosis deformity carries a risk of progression with time, being a female with Cobb angle > 30 degree carries the highest risk, with a 7–10:1 ratio compared to males [1, 9, 12].

AIS affects the quality of life of its patients, who can suffer from poor self-image and poor social function [13]. Patients may also have difficulty in the ability to move due to rib cage prominence, torso disfigurement, and shoulder and waist asymmetry [14]. In some severe cases with Cobb angles exceeding 60°–100°, AIS might affect the cardiac system and cause limitation to the total lung volume [6, 13, 15]. Scoliosis can occur as right thoracic scoliosis or left lumbar scoliosis or both, resulting in spinal lateral deformation as a C or S shape [3, 5, 6] (Fig. 1).

1.1 Etiology

The pathogenesis of AIS is not yet known [1, 6]. Screening for symptoms during childhood physical examination is the basis for diagnosis [6]. Most screened adolescents have some degree of non-progressive AIS (Cobb angle less than 10°), and approximately 2–3% are diagnosed to have clinically significant AIS with 10° or more spinal curvature [11, 14, 16]. Since the underlying causes are unknown, prevention is not a viable option. This makes early screening and diagnosis of high importance to decide the path of intervention and treatment, such as outpatient and out-physiotherapeutic rehabilitation, soft and hard bracing, and surgery in some extreme cases (Cobb angle more than 50) [1, 2, 6, 12, 14].

Treatment protocol planning mainly depends on accurate Cobb angle measurement, which is used for the quantitative assessment of the lateral curvature of the spine in the frontal plane. Physicians usually measure the spine curvature angle manually with the help of a protractor to make the diagnosis. Physicians determine the curvature location by assigning the superior and inferior vertebrae, and then drawing lines on the X-ray film to calculate the angle formed by the intersection of the lines (Fig. 2). This measurement is valuable in planning the monitoring and management of spine deformities, and determining the severity of the curvature [5, 10].

Despite the simplicity of the manual procedure for measuring the Cobb angle, the determination of the upper and lower vertebrae, drawing lines and calculating the angle could be sources of human error that will lead to intra- and inter-observant variability occurring at about 3°–5° and 6°–7°, respectively [1, 16, 17]. This might lead to inaccurate assessment of the patient, resulting in incorrect diagnosis and possible incorrect or delayed treatment.

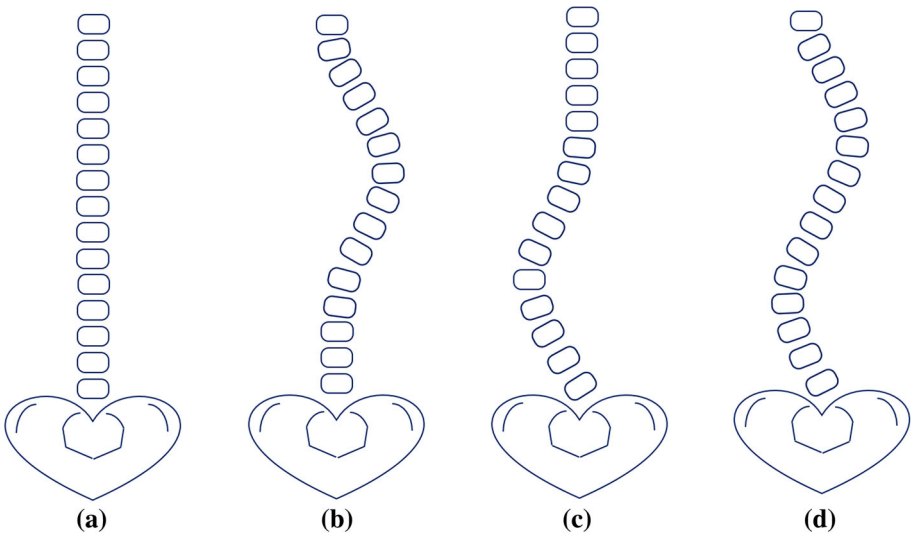

Fig. 1 Illustration showing the spinal lateral (2D) deformities associated with IS: **a** normal spine, **b** right thoracic scoliosis (C-shape), **c** left lumbar scoliosis (C-shape), and **d** right thoracic and left lumbar scoliosis (S-shape)

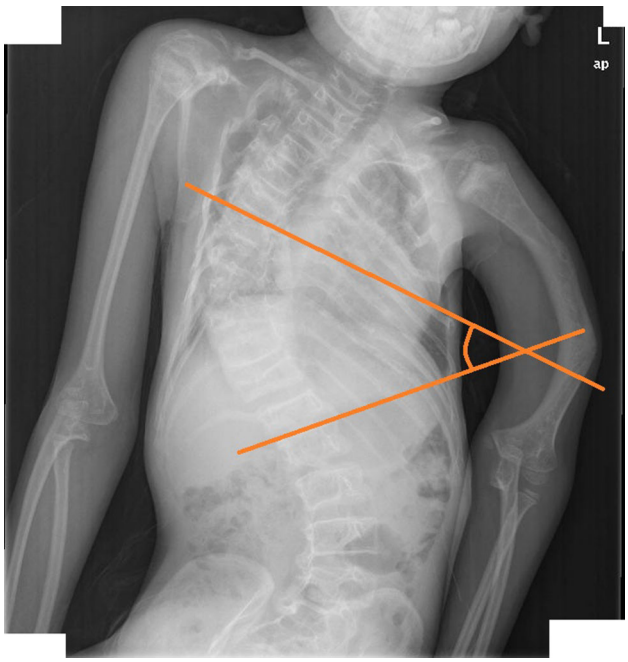

Fig. 2 Manual determination of the Cobb angle using upright X-ray frontal images. The physician determines the curvature location by assigning the posterior and inferior vertebrae and then draws lines on the X-ray film to calculate the angle formed by the intersection of the lines. Identifying information on the corners of the X-ray film was cropped prior to the start of the study

Adding to that, the time needed to measure the angle depends on the physician's experience and availability of specific tools (pins and goniometer) [4, 18]. Therefore, decreasing the inter- and intra-observer variability and the angle measuring time is needed. Hence, developing an accurate, standardized and automated computer-assisted method is desirable for screening and diagnostic application.

1.2 Current screening methods for automatic Cobb angle measurements

Shea et al. [19] reported a comparative study between computer-assisted measurement using a computer mouse on digital X-ray images and manual measurement on standard X-ray images. The study showed a decrease in the intra-observer variability by approximately 3° in computer-aided measurements compared to the manual ones. This was an early indication of the ability of computer-assisted measurements to eliminate intrinsic error arising from inaccurate manual protractor placement and the use of wide-diameter markers. Another study by Stokes and Aronsson [18] considered the reliability of the computer-assisted measurement protocol of the Cobb angle compared to unassisted observer measurements. They reported an inverse relationship between the repeatability and the time spent on image marking for the unassisted observer with no correlation with the image quality or curve magnitude. The algorithm presented was superior to previously published series.

The method presented by Illes et al. [7, 20] has been reported on a three-dimensional reconstruction of the X-ray images, in which a three-dimensional evaluation of the spinal curvature was compared to a two-dimensional evaluation, with very agreeable results. Although the method provides a true three-dimensional reconstruction and classification of scoliosis, its complexity and requirement of specialized imaging and processing methods render it more suitable for pre- and post-operation, compared to use for large-scale screening.

Other studies detailed by Langensiepen et al. [21] proposed different techniques to automatically measure the Cobb angle. However, user selection of the end point of the superior and inferior curvature vertebrae was needed to calculate the Cobb angle. Selecting the end point of the superior and inferior curvature vertebrae manually is a source of intrinsic, observer-introduced variability for Cobb angle measurement, when using either a manual or computer-aided methodology.

Sardjono et al. [3] proposed a modified charged-particle model to determine the curvature of the spine using three curve-fitting methods and compared them with the manual results from three observers. They reported better assessment results from the automated measurement of Cobb angle compared to the manual one. The initial particle position can be defined manually or automatically. They showed that both the piecewise linear with 3-segment and the polynomial of order 6 are better than splines curve-fitting in terms of absolute mean error and standard deviation. However, in their work, they needed to divide the spine into 2 or 3 parts with equal particle numbers, based on the C or S spine curvature, consecutively. Nevertheless, the charge of the electrical field used in their model was based on gray-scale level on the image, which can vary according to patients position and imaging setups. On the other side; in their polynomial fitting of order 6; they rely on the readings mean abs error and standard deviation to report better Cobb angle assessment regardless of the goodness of fit.

In this paper, we propose and test an algorithm for a computer-aided program for automated Cobb angle measurement (ACAM) from digital X-ray images without the need for manual pre-marking of the end points of the superior and inferior vertebrae of the scoliosis curvature, or the need for the manual or automatic segmentation of the spine. The angles are measured automatically, without user a priori knowledge of the end-vertebrae location, or the C or S curvature classification of the IS.

2 Methodology

2.1 Patient recruitment and demographics

A series of 47 upright, anterior–posterior radiographs from patients diagnosed with AIS was obtained to test the proposed algorithm. Images were collected at King Hussain Medical Center, Royal Medical Services (RMS), Amman, Jordan. The local institutional review board (IRB) approved the protocol, and signed consents for participation in the study were acquired from the patients' legal guardians.

Out of the 47 radiographs, 19 images were excluded due to low contrast of the image or the presence of metal in clothing. It is worthy to note here that due to local cultural restrictions, it is common for females to refuse removal of all clothes during the conduction of medical tests, causing metallic items to remain in the clothing. The remaining patient pool of 28 patients included 14 females and 14 males with average lateral spinal curvatures ranging from manually measured Cobb angles of 10°–98° (Table 1). The patients were between 10 and 18 years old with an average age of 15.6 ± 1.3 years.

2.2 Manual Cobb angle measurement method

Three manual measurements were obtained using the X-ray images performed by a spine orthopedic surgeon, a pediatric orthopedic surgeon, and the first author of this study (a biomedical engineer who was trained to perform the manual measurement). The manual measurements were taken in a blinded fashion.

The manual Cobb angle measurements were taken on raw digital radiographs using an in-house image analysis software program. This software helps the user to select points representing the superior and inferior curve vertebrae and to create lines between them. The software calculates the angles at the intersection of these lines. The two physicians and the first author performed the manual Cobb angle measurements based on this standard protocol. Moreover, this software calculation of the angles is completely dependent on the points location chosen by the user for the superior and inferior curve vertebrae, which caused user variations in angles calculation.

2.3 Proposed ACAM method

In our proposed ACAM method, we aimed at having minimal manual intervention by the user to determine the Cobb angles in the X-ray image. The algorithm was developed using MATLAB R2016a (MathWorks, Natick, MA). The method includes two phases: image preparation and angle measurement. Figure 3 is a block diagram summarizing the proposed algorithm steps. We must point out that a priori knowledge for a C or S curvature is not required during the performance of these steps. We detail hereafter the steps performed within each phase:

Table 1 Subject demographics and mean Cobb angle measurements

Subject#	Gender	Age	Cobb angle measurement
1	F	15	35 ± 3.1
2	M	16	30 ± 0.0
3	F	15	61 ± 1.7
4	M	16	38 ± 2.7
5	F	17	46 ± 2.7
6	M	16	37 ± 7.5
7	M	16	31 ± 8.5
8	M	16	84 ± 14.6
9	F	16	13 ± 2.1
10	F	16	47 ± 5.7
11	F	16	57 ± 7.6
12	F	16	49 ± 3.1
13	F	16	36 ± 5.1
14	M	15	24 ± 3.8
15	F	16	35 ± 9.6
16	F	16	15 ± 0.0
17	M	16	10 ± 0.0
18	M	15	50 ± 4.0
19	M	16	43 ± 1.7
20	F	18	28 ± 4.2
21	M	16	32 ± 2.1
22	F	17	24 ± 5.3
23	M	15	35 ± 2.1
24	F	15	40 ± 3.2
25	F	16	98 ± 18.3
26	M	15	38 ± 9.0
27	M	10	68 ± 4.6
28	M	15	40 ± 5.1
	14 females	15.6 ± 1.3 years	
	14 males		

2.3.1 Phase 1: image preparation

(a) Importing the raw digital X-ray image into MATLAB (see Fig. 4a).
(b) Converting the image to an 8-bit, 256 gray-scale level image.
(c) Rotating the image horizontally (see Fig. 4b).
(d) Manual cropping of edges of the image to select the spinal cord only, the new image size (M rows× N columns). This is the only step that requires user input in the algorithm. It does not

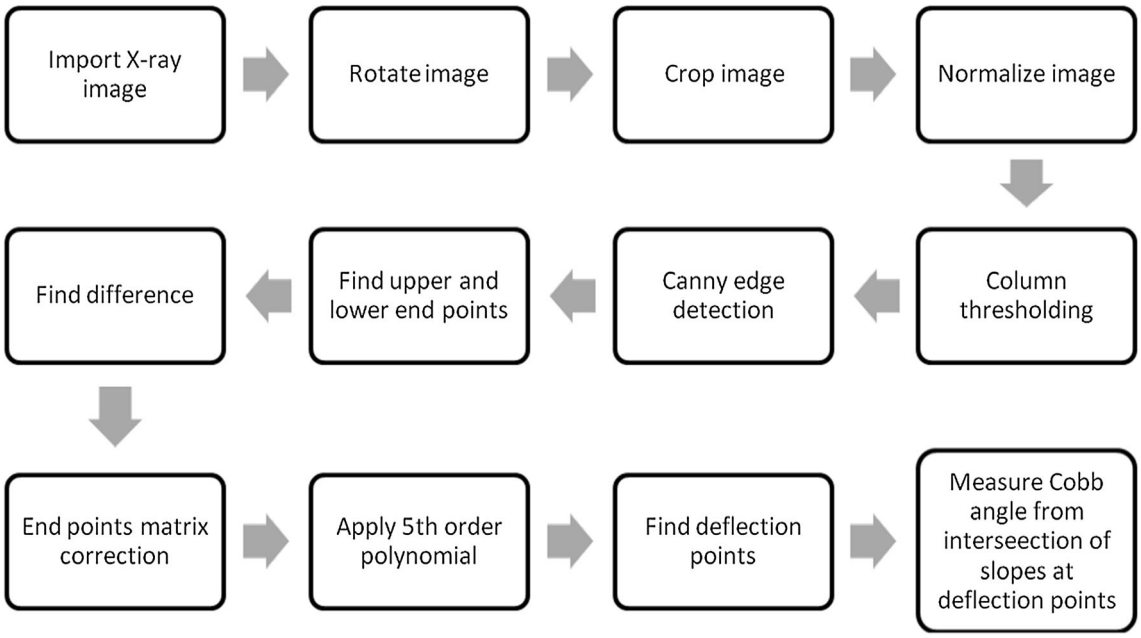

Fig. 3 Block diagram of the proposed ACAM

require a priori knowledge of the type of scoliosis (S or C curvature), or any requirement to assign the curve vertebrae end points (see Fig. 4c). Note that this is only needed if the image was large than the spinal region.

(e) Normalizing each image to its maximum intensity value.

(f) For each column in the image (along the lateral section of the image), the average value (avg_i) and the standard deviation (std_i) of the gray-level values are calculated, where i ranges from 1 to N, and N is the total number of column in the image. A column thresholding was applied to each column of the cropped image results from step d. The value of the threshold for column i is

$$\text{Th}_i = \text{avg}_i + \text{std}_i. \quad (1)$$

Hence, any pixel in column i with intensity less than the Th_i value will be assigned a zero; otherwise, it will keep its original signal intensity (see Fig. 4d).

(g) Apply Canny edge detection to find the spine edges (see Fig. 4e).

2.3.2 Phase 2: angle measurement

Applying phase 1 produces a binary matrix with M rows and N columns. Each column is mostly made up of zero values, and a group of 1's that represent the general location of a slice of the spine within that column.

(a) For each column in the matrix, the location of the upper and lower pixel (i.e., the first and last) for the 1 value pixels is calculated. The (x_u,y_u) and (x_l,y_l) locations of these pixels are stored in the lower and the upper end point matrices. This process is repeated for all columns $1 \leq i \leq N$.

(b) For each column (y_i) in the matrix, the difference between (x_u) and (x_l) is calculated and stored ($diff_i$). This process is repeated for all columns $1 \leq i \leq N$. The average value (diff − avg) and the standard deviation (diff − std) of the difference values are calculated, and the following loop is then applied on the lower and the upper end point matrices, respectively:

For $1 \leq i \leq N$
  if the $diff_i >= (diff\text{-}avg + 2^* \ diff\text{-}std)$
    $(x_u,y_u)=(x_l,y_l)\text{-}diff\text{-}avg$;
  else
    $(x_u,y_u)(x_u,y_u)$;

For $1 \leq i \leq N$
  if the $diff_i >= (diff\text{-}avg)$
    $(x_l,y_l)=(x_u,y_u)+diff\text{-}avg$;
  else
    $(x_l,y_l)=(x_l,y_l)$;

These values for thresholding were selected by applying several trials until the one with the best

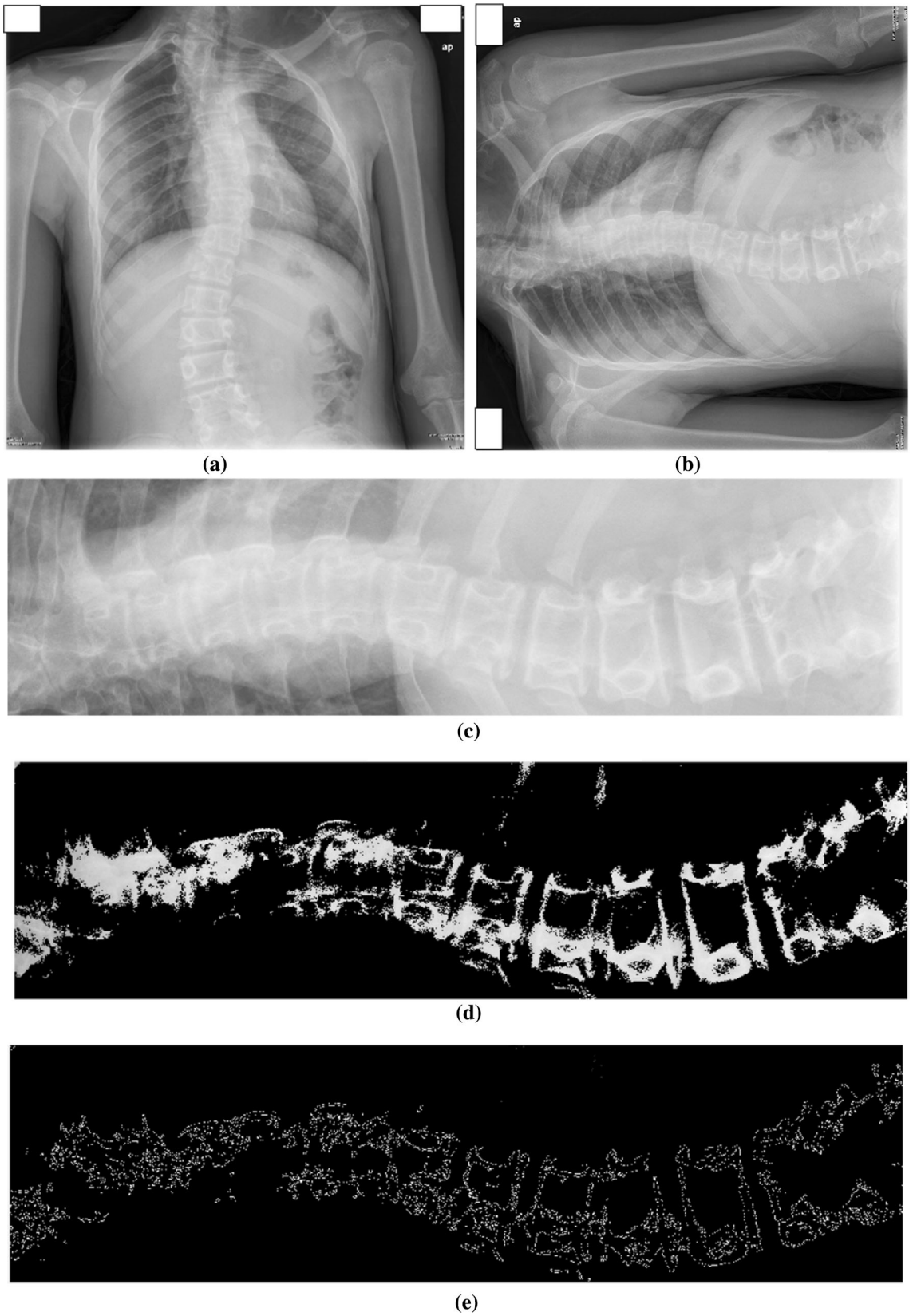

Fig. 4 Results from applying phase 1 on the X-ray image. **a** Row image. **b** Rotated image. **c** Cropped image. **d** Applying column thresholding. **e** Applying canny edge detection

results was found. A new difference between the new (x_u) and the new (x_l) is calculated and stored as a new (diff$_i$). This process is repeated for all columns $1 \leq i \leq N$. The average value (diff − avg) and the standard deviation (diff − std) of the new difference values are calculated and the above-described process is repeated again.

(c) From the resulting (x_u,y_u) and (x_l,y_l), the middle point is calculated (x_m,y_m):

$$(x_m, y_m) = (x_u, y_u) + (\text{diff} - \text{avg}/2) \tag{2}$$

(d) A fifth-order polynomial curve is then fitted through the stored locations (x_m,y_m), see Fig. 5. The rationale for the selection of a fifth-order polynomial as a minimum order is to assure the presence of 3 deflection points within the viewing area, accounting for C- or S-shape scoliosis.

(e) Starting with a fifth-order polynomial of the form

$$y = a_0x^5 + a_1x^4 + a_2x^3 + a_3x^2 + a_4x + a_5 \tag{3}$$

we can find the x-axis location of the deflection points by solving the roots of the second ordered derivative of the function in (3) as follows:

$$\frac{d^2y}{dx^2} = 0 \tag{4}$$

Our curve fitting was not restricted to the cropped image borders to insure the best goodness of fit; therefore, roots (i.e., x-axis locations) can either be inside or outside the image dimension. After deleting the repeated roots, 4 possible cases may occur in which 0, 1, 2, or 3 roots will be inside the image dimension and the other roots outside the image dimension. Figure 6 shows how this issue was tackled in our algorithm. In the case of 3 roots inside the image dimension, we simply find the two angles from the 3 deflections points. If there are only 2 roots inside the image dimension and no other root is outside the image dimension, we consider the first and the last points of the image as another 2 deflection points and we calculate 3 angles from the 4 deflection points and then choose the larger 2 angles. Another option included is if there are only 2 roots inside the image dimension and 1 other root outside the image dimension. We then select either the first or the last points of the image, depending on the closest root location. The third case is if there is only 1 root inside the image dimension. We then consider the first and last points of the image as the other 2 deflection points and we calculate 2 angles from the 3 deflection points. The last case is when NO root is inside the image dimension. In this case, an error message will appear to the user. This case did not happen for any recruited subject.

(f) Once the x-axis location of the deflection points is found, we can calculate the Cobb angle by finding the angle between the lines orthogonal to the tangents of the fifth-order polynomial fitted curve at the deflection points. The first angle is calculated

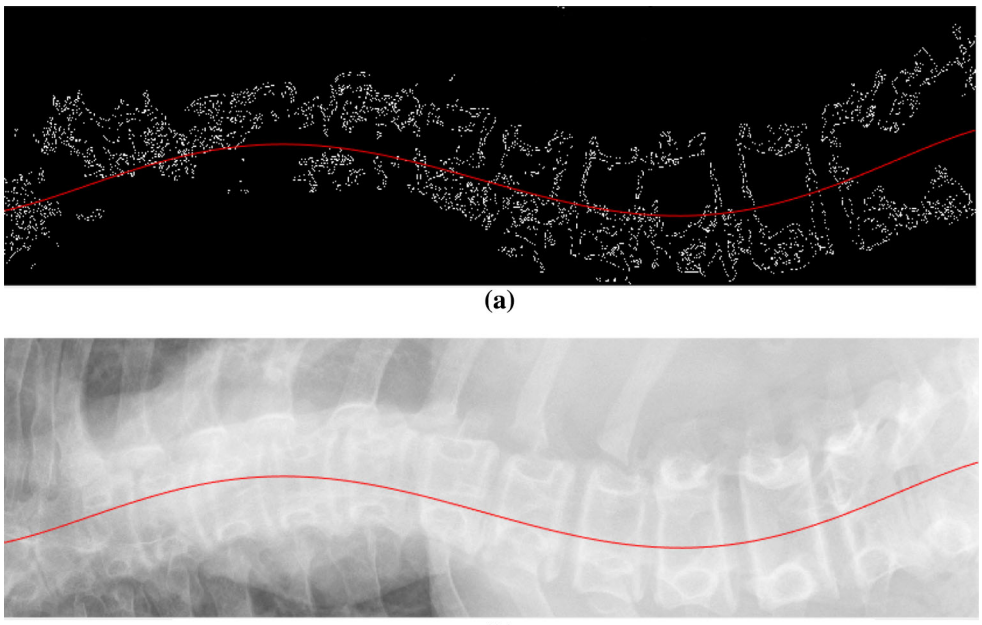

Fig. 5 Results from applying phase 2 on the X-ray image. A fifth-order polynomial curve is then fitted through the stored locations for (x_m,y_m). **a** Fifth-order fit for the 3 lines at the processed image. **b** Fifth-order fit for the 3 lines at the cropped image

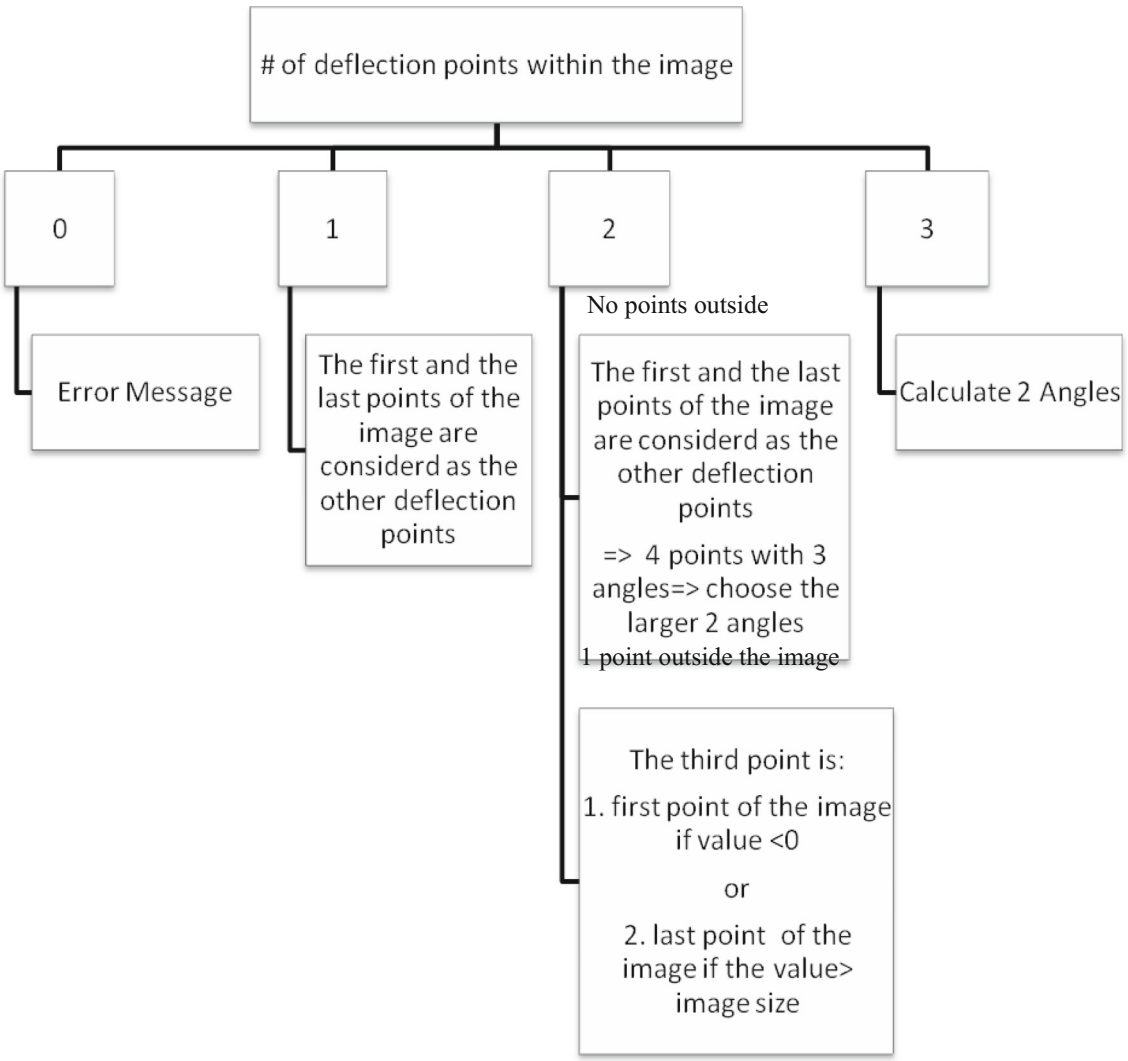

Fig. 6 Block diagram of the 4 different cases that might appear while fitting the spin into fifth-order polynomial to find the 3 deflection points in order to calculate Cobb angle

for the first and second deflection points. The second angle is calculated for the second and third deflection points. The larger of the two resultant angles are assigned as the Cobb angle for the image. See Fig. 7.

3 Results

Assessment of the Cobb angle was performed using a manual method (3 observers blinded from each other's readings) and our proposed computerized method (ACAM). The results from applying our proposed ACAM

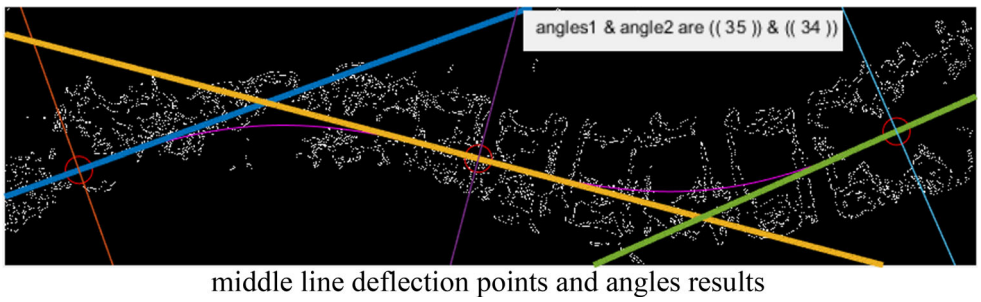

Fig. 7 Angle calculations from the three deflection points. The first angle is calculated for the first and second deflection points. The second angle is calculated for the second and third deflection points for the middle fitted fifth-order polynomial

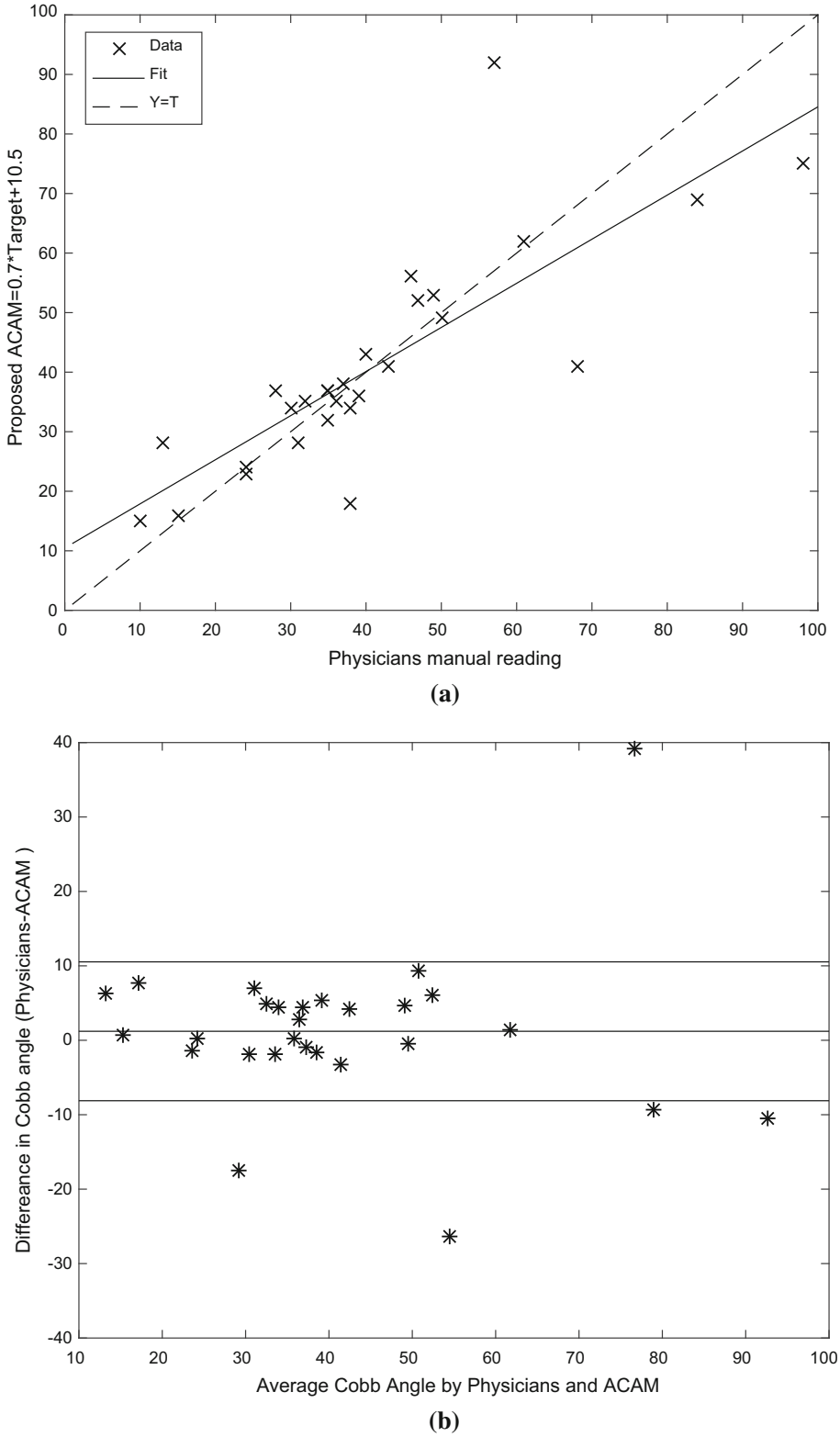

Fig. 8 **a** Linear regression plot depicting the relationship between the manual measurements of the Cobb angle, and the results obtained from the proposed ACAM method. **b** Measuring agreement between the manual and the proposed ACAM in Cobb angle measurements. Three lines representing the mean, the mean $-$ 2 * std and mean $+$ 2 * std were added to the plot. The outer two lines represent the limits of agreement (i.e., 95% confident interval)

on the recruited scoliosis patients versus the mean of the manual measurements are shown in Fig. 8a. The proposed method correlates with the manual measurements, with an *r*-Pearson correlation coefficient of 0.81. The linear regression equation between the manual measurements (*x*-axis) and the output of the proposed ACAM (*y*-axis) is ACAM results = 0.74 * (mean of manual readings) $+$ 10.5.

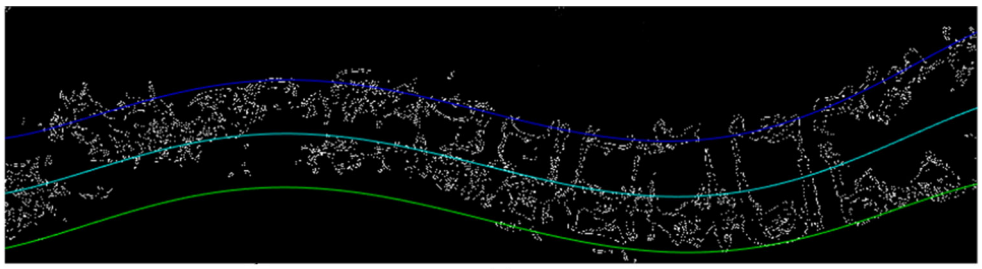

(a)

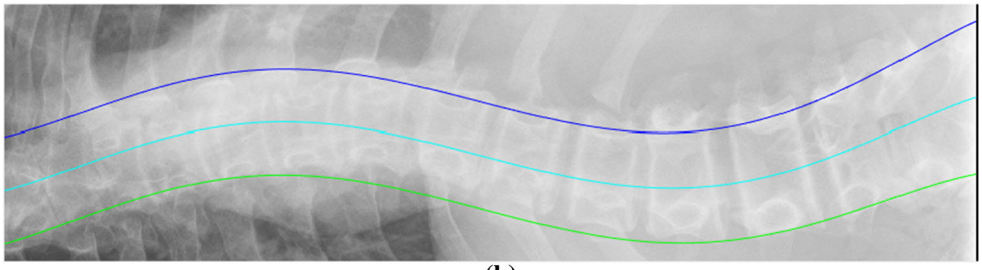

(b)

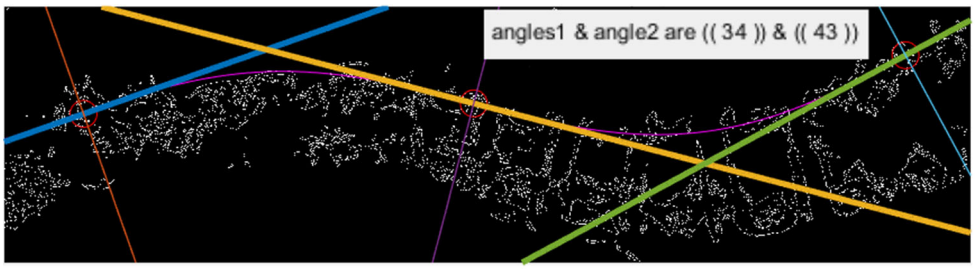

(c)

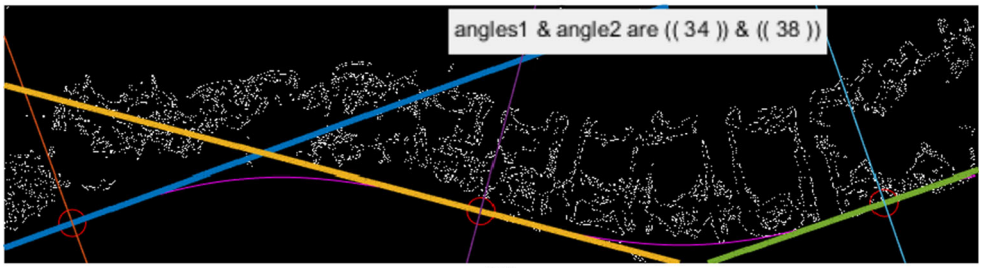

(d)

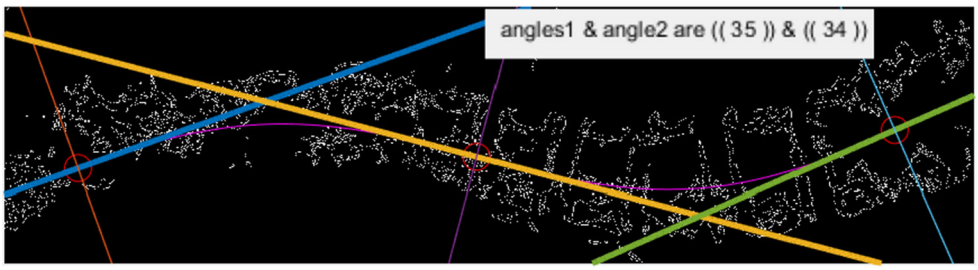

(e)

Fig. 9 Results from applying phase 2 on the X-ray image. A fifth-order polynomial curve is then fitted through the stored locations for (x_u,y_u), (x_l,y_l) and (x_m,y_m) and produce 3 polynomials that were used to calculate the Cobb angle from the 3 deflection points in each fit. **a** Fifth-order fit for the 3 lines at the processed image. **b** Fifth-order fit for the 3 lines at the cropped image. **c** Upper line inflection points and angle results. **d** Lower line inflection points and angle results. **e** Middle line inflection points and angle results

To measure the agreement between the manual and the proposed ACAM in Cobb angle measurements, the method proposed in [22] was adopted and the results are shown in Fig. 8b. The average and the STD of the difference between the manual and ACAM readings were − 1.21 and 4.66, respectively. Three lines representing the mean, the mean − 2 * std and mean + 2 * std were added to the plot. The outer two lines represent the limits of agreement (i.e., 95% confident interval).

Table 2 Upper, lower, and middle fit from ACAM measurements repeated 10 times on all recruited subjects

Subject#	Upper fit mean + STD	Lower fit mean + STD	Middle fit mean + STD	Average reading of fits together
1	31 ± 2.2	34 ± 1.2	33 ± 2.4	33 ± 2.0
2	37 ± 2.3	35 ± 4.0	35 ± 1.6	35 ± 2.7
3	61 ± 1.2	65 ± 1.2	63 ± 1.2	63 ± 1.2
4	23 ± 3.6	19 ± 3.4	20 ± 3.5	20 ± 3.5
5	55 ± 3.0	56 ± 2.4	55 ± 2.4	55 ± 2.6
6	44 ± 5.3	41 ± 3.0	42 ± 3.7	42 ± 4.0
7	30 ± 1.7	29 ± 2.1	29 ± 1.6	29 ± 1.8
8	74 ± 5.9	76 ± 2.4	74 ± 4.2	74 ± 4.2
9	15 ± 2.7	22 ± 3.0	21 ± 5.6	19 ± 3.8
10	53 ± 1.8	50 ± 1.7	51 ± 1.4	52 ± 1.6
11	99 ± 4.6	92 ± 3.4	96 ± 3.4	96 ± 3.8
12	52 ± 1.3	62 ± 3.6	55 ± 3.3	57 ± 2.7
13	34 ± 1.1	38 ± 1.3	36 ± 1.1	36 ± 1.1
14	26 ± 2.3	22 ± 0.6	23 ± 0.7	23 ± 1.2
15	41 ± 1.8	35 ± 1.8	38 ± 1.5	38 ± 1.7
16	16 ± 0.5	16 ± 0.8	16 ± 0.5	16 ± 0.6
17	15 ± 1.9	18 ± 1.4	16 ± 1.5	16 ± 1.6
18	50 ± 0.3	49 ± 0.7	49 ± 0.4	49 ± 0.5
19	38 ± 4.0	42 ± 2.2	40 ± 2.9	40 ± 3.0
20	36 ± 3.1	35 ± 6.9	35 ± 4.2	35 ± 4.7
21	35 ± 2.2	38 ± 2.0	36 ± 2.1	36 ± 2.1
22	25 ± 0.3	24 ± 0.3	24 ± 0.7	24 ± 0.4
23	41 ± 1.5	36 ± 2.8	39 ± 3.2	39 ± 2.5
24	39 ± 2.2	37 ± 2.5	38 ± 2.5	38 ± 2.4
25	107 ± 10.7	85 ± 11.9	87 ± 9.9	93 ± 10.8
26	39 ± 4.2	37 ± 3.0	37 ± 2.8	37 ± 3.3
27	42 ± 0.6	40 ± 0.6	41 ± 0.6	41 ± 0.6
28	43 ± 2.8	44 ± 3.4	45 ± 4.9	44 ± 3.7
STD	2.67	2.62	2.64	2.64

3.1 Upper, lower or middle fifth-order polynomial

To examine the Cobb angle results obtained from the upper and lower side points of the spine to that obtained from the middle points of the spine used above, steps d through f, of processing phase 2, were applied again. Another two fifth-order polynomial curves using the stored locations for (x_u,y_u) and (x_l,y_l) were generated, representing the upper and lower fit of the spin. The x-axis locations of the deflection points are then found, and the Cobb angle is calculated as described in the methodology above. Figure 9 shows the results of fifth-order polynomial curve fitting of the upper, lower and middle fit of the spin. The ACAM was then randomly repeated 10 times on all recruited subjects, and the Cobb angle results from using (x_u,y_u) and (x_l,y_l) were compared to the results from the middle fit of the spin using (x_m,y_m). Results from the upper, lower and middle fit of the spin are shown in Table 2. The STD of Cobb angle measurements for all 28 subjects was 2.67°, 2.62° and 2.64° for the upper, lower and middle fit of the spine, respectively. The average accuracy was 84, 82 and 83% for the upper, lower and middle fit of the spine, respectively, compared to the manual results. Notice that the results from the three fits are very comparable, with the middle fit located intermediate in terms of STD and accuracy compared to the upper (which have a slightly higher STD and accuracy) and lower (which have a slightly lower STD and accuracy) spin fit. Therefore, the middle fit was selected.

3.2 Sixth- and seventh-order polynomial

We investigated if using a higher-order polynomial would produce more accurate results compared to the fifth-order calculations or not. Step e, of phase #2, was repeated for sixth- and seventh-order polynomials on all recruited X-ray images. Figure 10 shows the fitting result for subject #6.

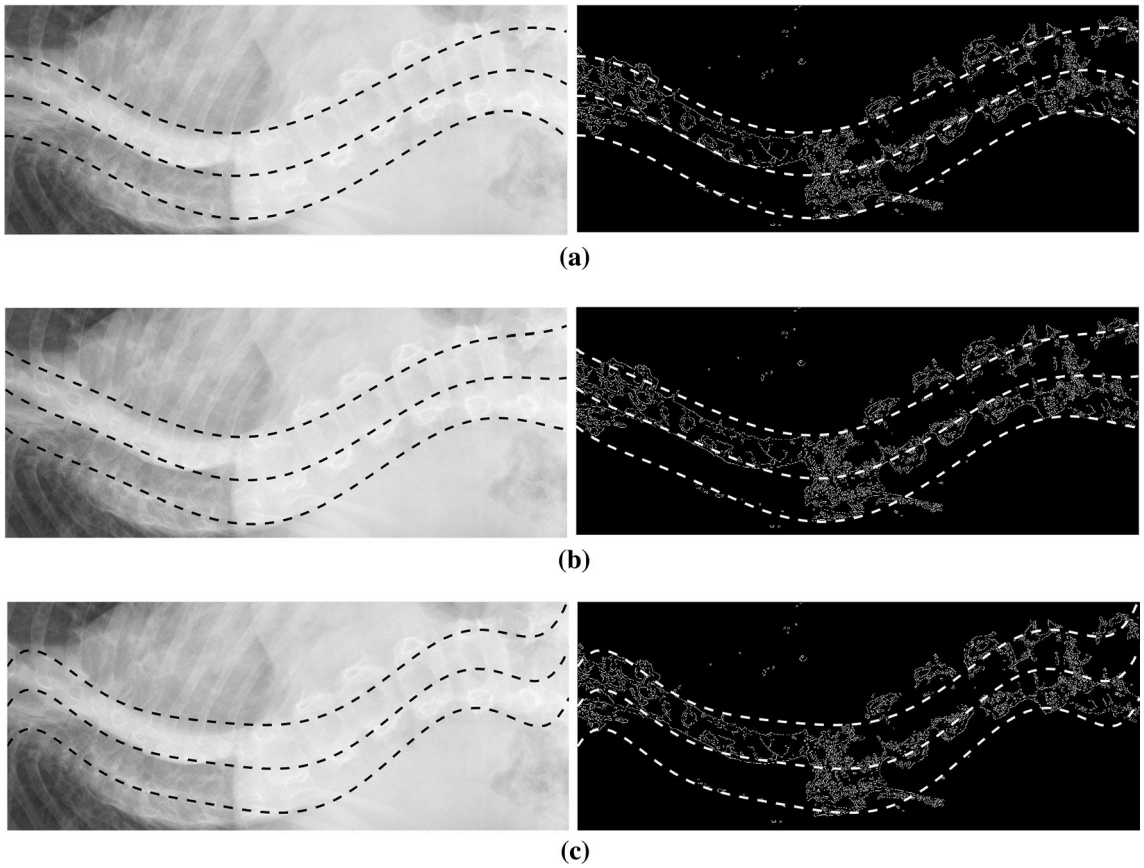

Fig. 10 Fitting results for **a** Fifth-, **b** sixth- and **c** seventh-order polynomials for subject #6 on raw and processed images, respectively

Note that the sixth-order polynomial showed more fluctuation on the fit compared to the fifth, and the seventh-order polynomial showed an even worse fit compared to the sixth- and fifth-order polynomials.

To give a clear assessment of the result, the fitting outputs were graded from grade 0 (representing a bad fit) to grade 5 (representing a perfect fit). The results from the sixth- and the seventh-order polynomial were compared to the fifth-order polynomial and are shown in Table 3. The results show better and more accurate curve fitting using the fifth-order polynomial compared to the sixth and seventh order, respectively, where the function became more squiggly as the order of the polynomial increases due to the presence of more deflection points in the function. This might be due to the shape of the scoliosis curvature, which has three deflection points. This can be satisfied by the fifth-order polynomial function with minimum fitting error compared to the others.

4 Discussion and conclusions

Selection of the upper and lower end-plate vertebrae for scoliosis assessments has been known to be a source of error in measuring the exact value of the Cobb angle [21]. Errors in Cobb angle estimation lead to inter- and intra-observer variations and, therefore, can lead to misdiagnosis and subsequent treatment failure. Therefore, many studies proposed a computer-assisted method to estimate Cobb angle [16–19] and gave the first indication for a more reproducible measurements and decreased the inter- and intra-observer variations. The proposed algorithm aims to minimize the error in estimating the Cobb angle by automatically fitting the spine curvature with a fifth-order polynomial, allowing for three deflection points to represent the spine general structure, and modeling of both C- and S-shape deformities associated with AIS.

The algorithm shows that the upper and lower end-plate vertebrae, which have the most deformity (mathematically called deflection points), can be detected automatically, and the intersection of the tangent lines of these deflection points can be used to determine the Cobb angle.

The algorithm was tested on X-ray images from 28 subjects (14 females and 14 males, average age of 15.6 $\pm$ 1.3 years) diagnosed with AIS. To estimate the accuracy of the proposed algorithm, three manual measurements were obtained by two physicians and a trained biomedical engineer, with manually measured Cobb angles ranging from of 10° to 98° for the test group. Measuring

Table 3 Fitting assessments for the fifth-, sixth- and seventh-order polynomials. The fitting assessments were graded from grade 0 (representing a bad fit) to grade 5 (representing a perfect fit)

Subject#	Fifth order	Sixth order	Seventh order
1	4	4	2
2	5	2	1
3	4	0	0
4	5	4	4
5	4	3	2
6	5	4	2
7	4	3	2
8	4	3	1
9	4	3	3
10	5	3	3
11	4	1	0
12	5	3	3
13	4	3	2
14	5	3	2
15	5	4	3
16	4	3	3
17	4	3	3
18	5	4	4
19	5	4	3
20	4	2	1
21	5	4	3
22	5	4	2
23	4	3	1
24	5	4	3
25	4	3	2
26	4	1	1
27	3	2	2
28	5	4	3
Average ± STD	4.43 ± .57	3.00 ± 1.05	2.18 ± 1.06

the Cobb angle with our proposed algorithm showed an acceptable correlation with the manual measurements with correlation factor (R) was equal to 0.81. The mean of the standard deviation of the manual readings and the algorithm results was 5.28° and 2.64°, respectively, and mean absolute error of 6.6°. This algorithm mean standard deviation is superior compared to other values in the literature [3, 21]. Nevertheless, our work is also superior and more simplified when compared to other studies considering the 3D vertebra vector curvature methods [7, 20] where they showed a very close relationship between the conventional manual 2D and their results.

The algorithm results can be enhanced if we consider the effect of scoliosis' location in the spine [23]. Noting that when the scoliosis curvature is located at the thoracic or lumbar spine region, ACAM provides reproducible result (for example, subjects #16, #18, and #22 with STD < 1 and accuracy $> 90\%$) compared to other cases when the scoliosis curvature is located at the cervical region of the spine, where high signal-intensity bones (i.e., clavicle) are included in the ROI (for example, subjects #4 and #27) compared to the manual reading. On the other hand, subjects with very large scoliosis curvature also show a high variability in Cobb angle values due to the displacement of the spine touching the outer line of the rib cage (for example, subjects #11 and #25).

Excluding the cervical and rib cage touching scoliosis cases (subjects #4, #11, #25 and #27), the mean of the standard deviation of the manual readings and the algorithm results was 4.73° and 2.35°, respectively, with mean abs error of 3.78° and correlation factor (R) equal to 0.94 (see Fig. 11a). The measuring agreement [22] between the manual and the proposed ACAM in Cobb angle measurements is shown in Fig. 11b. The average and the STD of the difference between the manual and ACAM readings were 2.13 and 2.67, respectively. Notice the lower STD and lower range for limits of agreement after excluding the cervical and rib cage touching cases. This problem of high signal-intensity pixels can be reduced by using a hand-free cropping option; however, this step can increase user intervention.

To test the reproducibility of ACAM results and to check which spine fit (i.e., upper lower or middle) is better, ACAM was randomly repeated 10 times on X-ray images for the recruited 28 subjects. Table 2 shows the Cobb angle results from the upper, lower and middle fit of the spin. The user needed to include the whole region of deformity, and to exclude the high signal-intensity regions from the neck, hips or ribs. While randomly applying the ACAM methodology, we tried to add or remove one vertebra after or before the most tilted vertebra. The mean value of STD of Cobb angle measurements for all 28 subjects was 2.67°, 2.62° and 2.64° for the upper, lower and middle fit of the spine, respectively, indicating a very good reproducibility from the three spinal fits.

Another topic of interest is what would result if we used a higher-order polynomial. Table 3 shows the results of measuring the Cobb angle using fifth-, sixth- and seventh-order polynomials. The results show better and more faithful spine representation using the fifth-order polynomial compared to the sixth and seventh order, respectively, where the function became more squiggly as the order of the polynomial increases due to the presence of more deflection points in the function. This might be due to the shape of the scoliosis curvature, which has three deflection points. This can be satisfied by the fifth-order polynomial function with minimum fitting error compared to the sixth- and seventh-order polynomials, which disagree with other studies [3].

Image standardization and minimal user intervention are a very important issue to decrease the results variation and

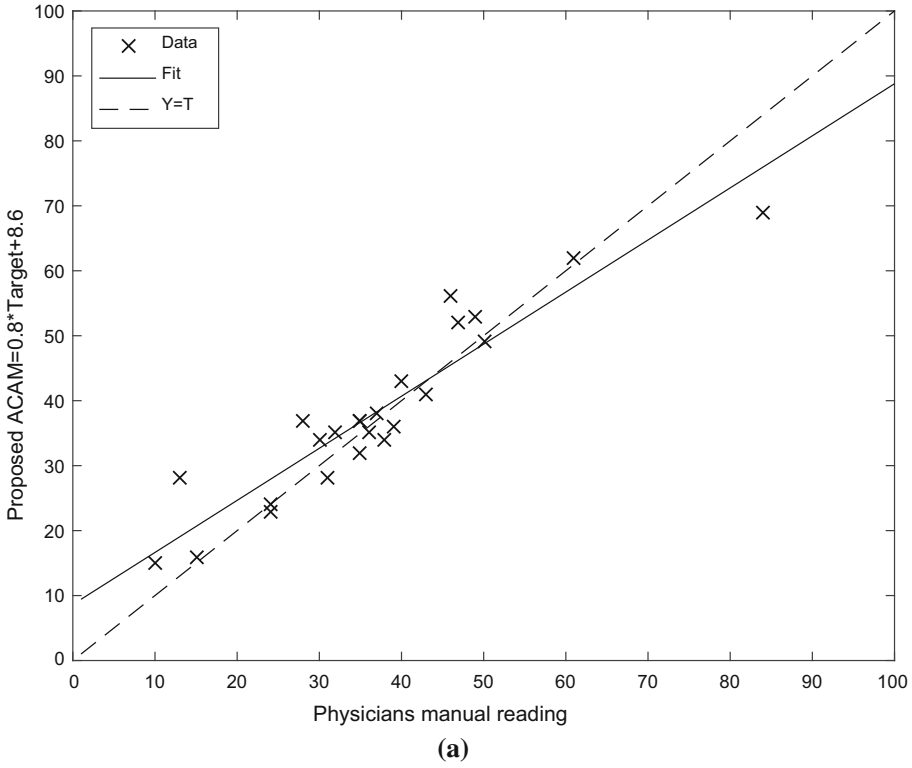

(a)

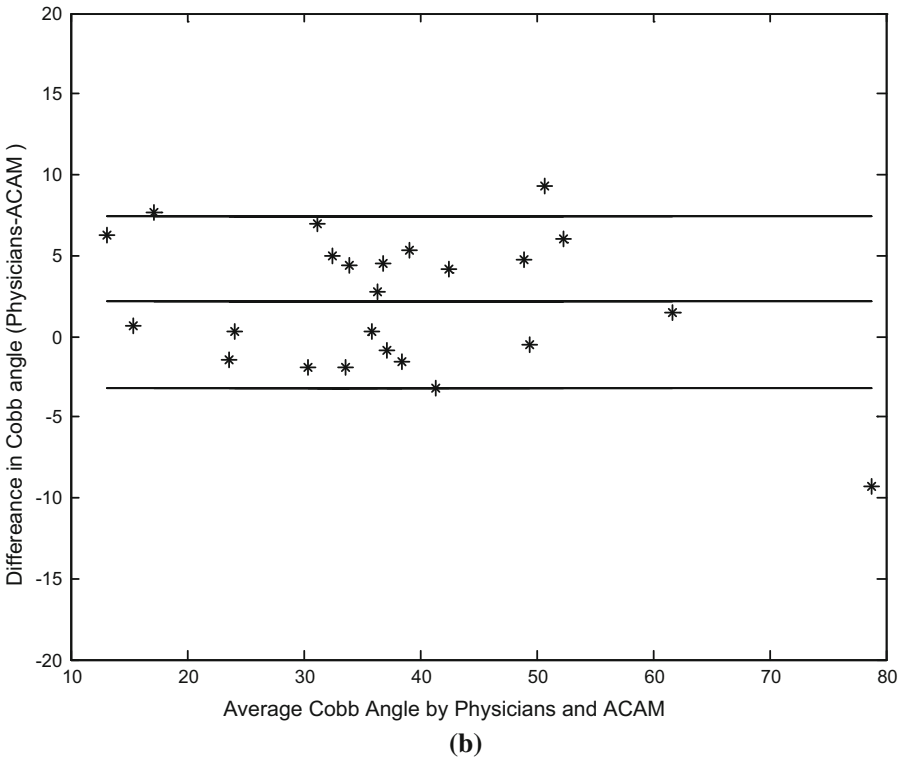

(b)

Fig. 11 **a** Linear regression plot depicting the relationship between the manual measurements of the Cobb angle, and the results obtained from the proposed ACAM method after removing subjects #4, #11, #25 and #27. **b**. Measuring agreement between the manual and the proposed ACAM in Cobb angle measurements after removing subjects #4, #11, #25 and #27. Three lines representing the mean, the mean $-$ 2 * std and mean $+$ 2 * std were added to the plot. The outer two lines represent the limits of agreement (i.e., 95% confident interval)

increase its reproducibility. Recall that 19 out of the 47 recruited radiographs were excluded due to low contrast or the presence of metal in clothing. For both reasons, the output of image thresholding will be affected and hence incorrect Cobb angle estimation will result. Therefore, image standardization and maintaining image collecting criteria are very important to decrease the ACAM percentage error and to insure wider use of it. In our proposed

algorithm, the only manual step is to crop the image to include the region of interest (ROI), which is the spine curvature. This step is only needed if the image was larger than spinal region. ROI selection in the image is not expected to affect the results reproducibility, as it neither requires a priori knowledge of the type of scoliosis (S or C curvature) nor need the user to choose the exact end-plate location. Therefore, this algorithm requires minimal training and experience to conduct and infer the results.

In conclusion, we propose an ACAM with an efficient algorithm for Cobb angle measurement from digital X-ray images of the spine that require minimal user input. It automatically estimates the Cobb angle by inserting the image path to the program, which requires no special skills from the user. This ACAM minimized and simplified user intervention by only selecting the spine curvature box, thus allowing for easier and more accurate measurements of Cobb angle and resulting in a shorter time to diagnosis.

References

1. Negrini S et al (2012) 2011 SOSORT guidelines: orthopaedic and rehabilitation treatment of idiopathic scoliosis during growth. Scoliosis 7(1):1–35
2. Clark EM et al (2014) Association between components of body composition and scoliosis: a prospective cohort study reporting differences identifiable before the onset of scoliosis. J Bone Miner Res 29(8):1729–1736
3. Sardjono TA et al (2013) Automatic Cobb angle determination from radiographic images. Spine 38(20):E1256–E1262
4. Kundu R, Chakrabarti A, Lenka PK (2012) Cobb angle measurement of scoliosis with reduced variability. arXiv preprint arXiv:1211.5355
5. Krishnan SP (2013) Scoliosis. In: Mohan Iyer K (ed) Trauma management in orthopedics. Springer, Berlin, pp 213–228
6. Hresko MT (2013) Idiopathic Scoliosis in adolescents. N Engl J Med 368(9):834–841
7. Illés T, Somoskeöy S (2013) Comparison of scoliosis measurements based on three-dimensional vertebra vectors and conventional two-dimensional measurements: advantages in evaluation of prognosis and surgical results. Eur Spine J 22(6):1255–1263
8. Abuzaghleh T, Barkana B (2012) Computer-aided technique for the measurement of the Cobb angle. In: Proceedings of the international conference on image processing, computer vision, and pattern recognition (IPCV). The Steering Committee of the World Congress in computer science, computer engineering and applied computing (WorldComp)
9. Konieczny MR, Senyurt H, Krauspe R (2013) Epidemiology of adolescent idiopathic scoliosis. J Child Orthop 7(1):3–9
10. Allen S et al (2008) Validity and reliability of active shape models for the estimation of Cobb angle in patients with adolescent idiopathic scoliosis. J Digit Imaging 21(2):208–218
11. Weiss H-R et al (2006) Indications for conservative management of scoliosis (guidelines). Scoliosis 1(1):1–5
12. Helenius I et al (2005) Does gender affect outcome of surgery in adolescent idiopathic scoliosis? Spine 30(4):462–467
13. Caronni A, Zaina F, Negrini S (2014) Improving the measurement of health-related quality of life in adolescent with idiopathic scoliosis: the SRS-7, a Rasch-developed short form of the SRS-22 questionnaire. Res Dev Disabil 35(4):784–799
14. Goldberg CJ et al (2008) Scoliosis: a review. Pediatr Surg Int 24(2):129–144
15. Huang J-Y, Kao P-F, Chen Y-S (2007) Automatic Cobb angle measurement system by using nuclear medicine whole body bone scan. In: MVA
16. Phan P et al (2011) Computer algorithms and applications used to assist the evaluation and treatment of adolescent idiopathic scoliosis: a review of published articles 2000–2009. Eur Spine J 20(7):1058–1068
17. Shea KG et al (1998) A comparison of manual versus computer-assisted radiographic measurement. Intraobserver measurement variability for Cobb angles. Spine (Phila Pa 1976) 23(5):551–555
18. Stokes IA, Aronsson DD (2006) Computer-assisted algorithms improve reliability of King classification and Cobb angle measurement of scoliosis. Spine 31(6):665–670
19. Shea KG et al (1998) A comparison of manual versus computer-assisted radiographic measurement—intraobserver measurement variability for Cobb angles. Spine 23(5):551–555
20. Illés T, Tunyogi-Csapó M, Somoskeöy S (2011) Breakthrough in three-dimensional scoliosis diagnosis: significance of horizontal plane view and vertebra vectors. Eur Spine J 20(1):135–143
21. Langensiepen S et al (2013) Measuring procedures to determine the Cobb angle in idiopathic scoliosis: a systematic review. Eur Spine J 22(11):2360–2371
22. Bland JM, Altmanab DG (2010) Statistical methods for assessing agreement between two methods of clinical measurement. Int J Nurs Stud 47(8):931–936
23. Wu W et al (2014) Reliability and reproducibility analysis of the Cobb angle and assessing sagittal plane by computer-assisted and manual measurement tools. BMC Musculoskelet Disord 15:33